

## Threshold electrodisintegration and electromagnetic form factors of the deuteron

R. Schiavilla

*Physics Division, Argonne National Laboratory, Argonne, Illinois 60439*

D. O. Riska

*Department of Physics, University of Helsinki, 00170 Helsinki, Finland*

(Received 29 August 1990)

The threshold electrodisintegration cross section and electromagnetic form factors of the deuteron are calculated by using the Argonne  $v_{14}$  model for the nucleon-nucleon interaction to generate the bound- and scattering-state wave functions. The exchange-current operator is constructed to be consistent with the interaction model. The calculated electrodisintegration cross section is in good qualitative agreement with the experimental data over the whole measured momentum-transfer range, and is sensitive to the electromagnetic form factors of the nucleon. The calculated form factors appear to be in good agreement with the empirical values, although uncertainties in the isoscalar model-dependent exchange-current contributions and nucleon electromagnetic form factors prevent definite predictions to be made at high values of momentum transfer. Finally, the cross section for radiative capture of thermal neutrons on protons is found to be within less than 1% of the measured value.

### I. INTRODUCTION

The cross section for backward electrodisintegration of the deuteron  $ed \rightarrow e'np$  near threshold and the electromagnetic form factors of the deuteron are the most obvious observables for testing models of the nucleon-nucleon interaction and the nuclear electroexcitation operator. Predictions of these operators within the usual nonrelativistic framework based on nucleonic degrees of freedom require, in addition to the model for the nucleon-nucleon interaction, a model for the electromagnetic form factors of the nucleon and, finally, a model for the exchange-current components associated with the nucleon-nucleon interaction.

Here we report a calculation of these observables, and the related cross section for radiative capture of thermal neutrons on protons, which is based on the Argonne  $v_{14}$  two-nucleon interaction.<sup>1</sup> The exchange-current operator is constructed to be consistent with this interaction apart from its purely model-dependent transverse parts, which we construct by considering standard meson-exchange mechanisms. In contrast to most earlier calculations, the present one is therefore based on a conserved current. For the electromagnetic form factors of the nucleon, we employ several different, but common, parametrizations in order to obtain a realistic estimate of the theoretical uncertainty limits of the predicted deuteron observables.

These can be summarized as follows. The calculated threshold electrodisintegration cross section at backward angles is in good qualitative agreement with the experimental data over the whole measured range of momentum-transfer values up to  $8 \text{ fm}^{-1}$ . At high values of momentum transfer our results are somewhat closer to the experimental data than those obtained with the Paris

model for the nucleon-nucleon interaction<sup>2</sup> in Ref. 3 (and later extended to higher values of momentum transfer, as reported in Ref. 4). However, with the present choice of nucleon electromagnetic form factors in the exchange-current operator, our results are clearly below the empirical values in the region around  $4 \text{ fm}^{-1}$  and somewhat too large in the region  $6\text{--}7 \text{ fm}^{-1}$ . It is worth noting that results that are in better agreement with the data over the whole range of momentum-transfer values have recently been obtained with an optimal version of the Bonn potential.<sup>5</sup> Our predicted cross section for radiative capture of thermal neutrons on protons (331.4 mb) is only 1% below the empirical value and, therefore, very satisfactory.

The calculated structure function  $A(q)$  of the deuteron, to which the two-body mechanisms mainly contribute a relativistic correction (evaluated here with a meson-exchange model), is in good agreement with the empirical values. The present predictions for the tensor polarization are qualitatively similar to earlier ones obtained with other potential models, but similar exchange-current contributions. The calculated values for the structure function  $B(q)$  follow the experimental data well, but have a large theoretical uncertainty at high momentum transfer, which is associated with the model-dependent  $\rho\pi\gamma$  exchange-current mechanism.

We give a complete graphical description of the contributions of the various dynamical mechanisms which affect the observables under consideration. The present calculation is similar in spirit to those reported in Refs. 3 and 6, but which used the parametrized Paris two-nucleon interaction.<sup>2</sup> The discrepancy between the present results and those obtained in Refs. 3 and 6 for the electrodisintegration cross section should, in spite of some differences in detail concerning the two-body exchange-current contributions, provide a measure of the

sensitivity to the nucleon-nucleon interaction model.

The paper is organized as follows. We describe the exchange-current and charge operators, and the methods used in the evaluation of the required matrix elements in Secs. II and III, respectively. The calculated results for the electrodisintegration cross section at threshold (and the related cross section for radiative neutron capture on protons) and electromagnetic form factors are reported in Secs. IV and V, respectively. Finally, in Sec. VI we present a concluding discussion, while in the Appendix we give the momentum-space expression for the  $\rho\pi\gamma$  current operator used in the present calculation, which includes corrections to the leading operator arising from the  $\rho$ -meson tensor coupling to nucleons. An abbreviated version of the electrodisintegration results has been presented in Ref. 7.

## II. ELECTROEXCITATION OPERATOR

The electromagnetic current operator of the two-nucleon system separates into a one-body and an irreducible two-body or exchange-current term. To establish our notation we note that the current operator of a single nucleon has the form

$$\begin{aligned} \mathbf{j}(\mathbf{q}) = & \frac{1}{4m_N} [G_E^S(q) + G_E^V(q)\tau_z](\mathbf{p}' + \mathbf{p}) \\ & + \frac{i}{4m_N} [G_M^S(q) + G_M^V(q)\tau_z]\boldsymbol{\sigma} \times \mathbf{q}. \end{aligned} \quad (2.1)$$

Here  $\mathbf{p}$  and  $\mathbf{p}'$  are the initial and final nucleon momenta and  $\mathbf{q} = \mathbf{p}' - \mathbf{p}$  is the momentum transfer to the nucleon. The nucleon mass is denoted  $m_N$  and the electromagnetic form factors of the nucleon are normalized as  $G_E^S(0) = G_E^V(0) = 1$ ,  $G_M^S(0) = 0.88$ ,  $G_M^V(0) = 4.706$ . For these nucleon form factors we shall employ the most common parametrizations used in the literature, which are those of Iachello, Jackson, and Lande (IJL),<sup>8</sup> Höhler *et al.*,<sup>9</sup> and Gari and Krüpelmann<sup>10</sup> (GK), and finally the dipole form  $\bar{D}$ , with inclusion of a neutron charge form factor that has the form<sup>11</sup>

$$G_E^n(q) = -\mu_n \frac{q^2}{4m_N^2} \frac{1}{1 + q^2/m_N^2} G_E^p(q), \quad (2.2)$$

with  $\mu_n = -1.913$ .

The exchange-current operator can be separated into a “model-independent” term which has to be consistent with the two-nucleon interaction so as to satisfy the continuity equation, and a purely transverse “model-dependent” term, which is unconstrained by the two-nucleon interaction.<sup>12</sup> The construction of the model-independent part of the exchange-current operator from the Argonne  $v_{14}$  potential has been described in Refs. 13 and 14. The model-dependent part of the exchange current operator is obtained by considering meson-exchange mechanisms as described below. The exchange-current operator used here is the same as that derived in Refs. 7 and 14.

The numerically most important part of the model-independent exchange-current operator is the isovector operator that is associated with the isospin-dependent

tensor and spin-spin interactions. This term, which has the isospin structure  $(\tau_1 \times \tau_2)_z$ , was originally derived by consideration of a simple pion-exchange mechanism,<sup>15,16</sup> but the resulting operator does not satisfy the continuity equation with a realistic potential model. The systematic method of generating this current operator from the Argonne  $v_{14}$  potential used in Refs. 13 and 14 involves separation of the isospin-dependent spin-spin and tensor potentials into terms that may be associated with the exchange of isospin one-pseudoscalar bosons (“generalized pion” exchange) and the exchange of isospin one-vector bosons (“generalized  $\rho$ -meson” exchange).<sup>17</sup> When these separated potential components are used in place of the simple pion and  $\rho$ -meson exchange potentials in the known expressions for the corresponding exchange-current operators, the resulting exchange-current operator satisfies the continuity equation with the realistic potential model (here the Argonne  $v_{14}$  interaction). The general expression for this exchange-current operator is given in Ref. 13.

To construct the exchange-current operator that satisfies the continuity equation with the spin-orbit interaction, one also has to consider the lowest-order relativistic correction to the nuclear charge operator, which leads to a commutator with the central potential that is of the same order  $(v/c)^2$  as the spin-orbit interaction.<sup>18</sup> We shall here use the method of Ref. 14 to construct this exchange-current operator. This is based on the assumption that the relevant scalar and vector meson-exchange-current operators can be generalized to a form which meets the requirement of current conservation with the Argonne  $v_{14}$  potential. The explicit form for this exchange-current operator is given in Ref. 14.

The construction of the exchange-current operators associated with the quadratic spin-orbit and  $L^2$  components of the interaction that is consistent with the form of meson-exchange-current operators would, in principle, require an expansion of the interaction and current operators to order  $(v/c)^4$ . However, here we shall be content to use an exchange-current operator constructed by direct minimal substitution in these interaction components as this procedure ensures that the continuity equation is satisfied [at least with the isospin-independent  $(\mathbf{L} \cdot \mathbf{S})^2$  and  $L^2$  components of the potential].

In addition to these exchange-current operators, which are required by the continuity equation, we also take into account the numerically most significant purely transverse “model-dependent” exchange-current operators. These are the pion-exchange-current and  $\rho$ -meson-exchange-current operators, which involve an intermediate  $\Delta_{33}$  resonance [Figs. 1(a) and 1(b)], and the  $\rho\pi\gamma$  and  $\omega\pi\gamma$  exchange-current operators [Fig. 1(c)]. The explicit expressions for these operators are given in Ref. 14, with the exception of that for the  $\rho\pi\gamma$  current which now includes previously neglected corrections arising from the tensor coupling of the  $\rho$  meson to the nucleon. The momentum-space structure of this operator is given in the Appendix. The numerical importance of these exchange current operators depends rather strongly on the coupling strength parameters for the meson-nucleon vertices as well as on how these vertices are cutoff at high

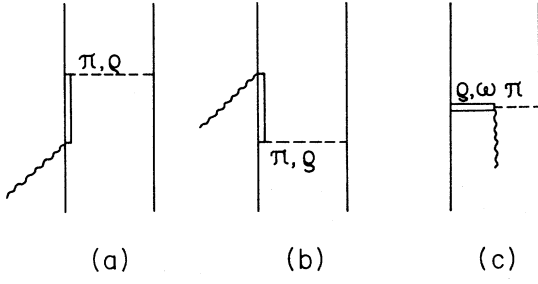


FIG. 1. Model-dependent exchange currents associated with the pion and  $\rho$ -meson excitation of intermediate  $\Delta_{33}$  resonances (a) and (b), and the  $\rho\pi\gamma$  and  $\omega\pi\gamma$  mechanisms (c).

values of momentum transfer.

We include cutoff factors of the usual monopole form at the meson-nucleon vertices with the cutoff masses 1.2 GeV/ $c^2$  for the  $\pi NN$  and 2.0 GeV/ $c^2$  for the  $\rho NN$  and  $\omega NN$  vertices. The  $\pi N\Delta$  and  $\rho N\Delta$  coupling constants are those obtained with the static quark model (with the large  $\rho NN$  tensor coupling constant value  $\kappa_\rho = 6.6$ ). For the  $\rho\pi\gamma$  and  $\omega\pi\gamma$  coupling constants, we use the values 0.56 and 0.63, respectively, as obtained from the widths of the radiative decays  $\rho \rightarrow \pi + \gamma$  (Ref. 19) and  $\omega \rightarrow \pi + \gamma$ .<sup>20</sup> Finally, vector meson pole term form factors are included at the  $\rho\pi\gamma$  and  $\omega\pi\gamma$  vertices, while the experimental transition form factor is used for the  $\gamma N\Delta$  vertex. The sensitivity to the cutoff parameters will be discussed in Secs. IV and V below.

As in the case of the current operator, the charge operator separates into one- and two-body terms. For the single-nucleon charge operator, we use the standard expression with the relativistic corrections included to lowest order<sup>21</sup>

$$\rho(\mathbf{q}) = \frac{1}{2} \left[ 1 - \frac{q^2}{8m_N^2} \right] [G_E^S(q) + G_E^V(q)\tau_z] - i \frac{\boldsymbol{\sigma} \cdot \mathbf{q} \times (\mathbf{p} + \mathbf{p}')}{16m_N^2} \{ [G_E^S(q) - 2G_M^S(q)] + [G_E^V(q) - 2G_M^V(q)]\tau_z \}. \quad (2.3)$$

While the main parts of the exchange current are linked to the form of the nucleon-nucleon interaction through the continuity equation, the most important exchange-charge operators are model dependent and may be viewed as relativistic corrections. There are nevertheless rather clear indications for their relevance from the failure of the impulse approximation in predicting the charge form factors of the three- and four-nucleon systems.<sup>22-24</sup>

Here we shall use the same model for the exchange-charge operator, which was recently employed in Ref. 24 in a study of the charge form factors of the bound trinucleons and four nucleons. This contains the pion-exchange-charge,  $\rho$ -, and  $\omega$ -meson-exchange-charge seagull (or "pair") operators that arise in the nonrelativis-

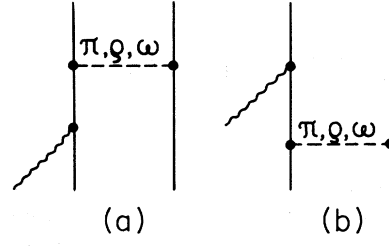


FIG. 2. Meson-exchange diagrams that involve the Born terms in the relativistic amplitudes for photoproduction of virtual mesons.

tic reduction of the Born term of the relativistic  $\pi$ -,  $\rho$ -, and  $\omega$ -meson photoproduction amplitudes (Fig. 2) and the charge components of the  $\rho\pi\gamma$  and  $\omega\pi\gamma$  mechanisms [Fig. 1(c)] considered above.

To reduce the model dependence of the pion-exchange-charge and  $\rho$ -meson-exchange-charge operators, we follow the procedure suggested in Ref. 24 and replace the meson propagators in the corresponding exchange-current operators by those constructed directly from the nucleon-nucleon interaction. The idea is the same as used in constructing the "generalized pion and  $\rho$ -meson" exchange-current operators described above by projecting out the components of the isospin-dependent spin-spin and tensor interactions, which correspond to exchange of  $0^-$  and  $1^+$  bosons. The explicit forms for the effective generalized pion and  $\rho$ -meson-exchange propagators are given in Eq. (3.5) of Ref. 24.

In the case of the  $\omega$ -meson-exchange-charge operator that corresponds to the diagrams in Fig. 2, we use an  $\omega$ -meson propagator that is multiplied by monopole form factors at the  $\omega NN$  vertices with the cutoff mass 2 GeV/ $c^2$ .

### III. CALCULATION

In the one-photon-exchange approximation, the inclusive electron scattering cross section is written as

$$\frac{d^2\sigma}{d\omega d\Omega} = \sigma_M [v_L R_L(q, \omega) + v_T R_T(q, \omega)], \quad (3.1)$$

where  $v_L$  and  $v_T$  are defined as

$$v_L = \frac{q_\mu^4}{q^4}, \quad (3.2)$$

$$v_T = tg^2\theta/2 + \frac{1}{2} \frac{q_\mu^2}{q^2}, \quad (3.3)$$

$q$  and  $\omega$  are the electron momentum and energy transfers, and  $q_\mu^2 = q^2 - \omega^2$  is the four-momentum transfer. The longitudinal and transverse response functions are given by

$$R_\alpha(q, \omega) = \frac{1}{2J+1} \sum_{M_j} \sum_f |\langle f | O_\alpha(\mathbf{q}) | i, JM_j \rangle|^2 \delta(\omega + E_i - E_f), \quad (3.4)$$

where  $i$  and  $f$  denote the initial and final states having energies  $E_i$  and  $E_f$ , respectively, and  $O_\alpha(\mathbf{q})$  is either the charge operator ( $\alpha=L$ ), or the transverse components of the current operator ( $\alpha=T$ ). For elastic scattering,  $f$  represents the initial state  $i$  recoiling with momentum  $\mathbf{q}$ .

We now specialize to the case of electrons scattering from the deuteron. The initial- and final-state wave functions are written as

$$|d, 1M_J\rangle = \left[ \frac{u(r)}{r} \mathcal{Y}_{011}^{M_J} + \frac{w(r)}{r} \mathcal{Y}_{211}^{M_J} \right] \eta_0^0, \quad (3.5)$$

$$|\mathbf{q}; \mathbf{p} S M_S T M_T\rangle = e^{i\mathbf{q}\cdot\mathbf{R}} \psi_{\mathbf{p}, S M_S T M_T}^{(-)}(\mathbf{r}), \quad (3.6)$$

respectively, where  $\mathbf{r} = \mathbf{r}_1 - \mathbf{r}_2$  and  $\mathbf{R} = \frac{1}{2}(\mathbf{r}_1 + \mathbf{r}_2)$  are the relative and center-of-mass coordinates, and  $\mathcal{Y}_{LSJ}^{M_J}$  are the spin-angle functions

$$\mathcal{Y}_{LSJ}^{M_J} = \sum_{M_L M_S} \langle LM_L, SM_S | JM_J \rangle Y_{LM_L}(\hat{\mathbf{r}}) \chi_{M_S}^S. \quad (3.7)$$

Here  $\chi_{M_S}^S$  and  $\eta_{M_T}^T$  are two-nucleon spin and isospin states, respectively. The ingoing scattering state of the two nucleons having relative momentum  $\mathbf{p}$  and spin-isospin states specified by  $SM_S TM_T$  is written as

$$\begin{aligned} \psi_{\mathbf{p}, S M_S T M_T}^{(-)}(\mathbf{r}) &= 4\pi \frac{1}{\sqrt{2}} \sum_{JM_J} i^L \delta_{LST} [Z_{LSM_S}^{JM_J}(\hat{\mathbf{p}})]^* \\ &\quad \times \frac{1}{r} u_{L'L}^{(-)}(r; p, JST) \mathcal{Y}_{L'SJ}^{M_J} \eta_{M_T}^T. \end{aligned} \quad (3.8)$$

Here we have used the notation

$$\psi_{\mathbf{p}, S M_S T M_T}^{(-)}(\mathbf{r}) \simeq \phi_{\mathbf{p}, S M_S T M_T}(\mathbf{r}) + 4\pi \frac{1}{\sqrt{2}} \sum_{JM_J} \sum_{LL'} i^L \delta_{LST} [Z_{LSM_S}^{JM_J}(\hat{\mathbf{p}})]^* \left[ \frac{1}{r} u_{L'L}^{(-)}(r; p, JST) - \delta_{L'L} j_L(pr) \right] \mathcal{Y}_{L'SJ}^{M_J} \eta_{M_T}^T, \quad (3.15)$$

so that interaction effects are retained in all partial waves with  $J \leq J_{\max}$ . For the threshold electrodisintegration, it was found that these interaction effects are negligible for  $J_{\max} > 2$ .

The response functions defined in Eq. (3.4) are given by

$$R_\alpha(q, \omega) = \sum_{S, T=0,1} R_\alpha^{ST}(q, \omega), \quad (3.16)$$

where the contributions from the individual spin-isospin states are

$$\delta_{LST} = 1 - (-)^{L+S+T} \quad (3.9)$$

and

$$Z_{LSM_S}^{JM_J}(\hat{\mathbf{p}}) = \sum_{M_L} \langle LM_L, SM_S | JM_J \rangle Y_{LM_L}(\hat{\mathbf{p}}). \quad (3.10)$$

The  $\delta_{LST}$  factor ensures the antisymmetry of the wave function, while the Clebsch-Gordon coefficients restrict the sum over  $L$  and  $L'$ . The radial functions  $u_{L'L}^{(\pm)}$  are related to those with outgoing-wave boundary conditions, denoted as  $u_{L'L}^{(\pm)}$ , via

$$u_{L'L}^{(-)}(r; p, JST) = [u_{L'L}^{(+)}(r; p, JST)]^*. \quad (3.11)$$

The  $u_{L'L}^{(\pm)}$  are obtained by solving the Schrödinger equation with the Argonne  $v_{14}$  interaction in the  $JST$  channel, and behave asymptotically as

$$\frac{1}{r} u_{L'L}^{(+)}(r; p, JST) \underset{r \rightarrow \infty}{\sim} \frac{1}{2} [\delta_{L'L} h_L^{(2)}(pr) + S_{L'L}^{JST} h_L^{(1)}(pr)], \quad (3.12)$$

where  $S_{L'L}^{JST}$  is the  $S$  matrix in the  $JST$  channel and the Hankel functions

$$h_L^{(1,2)}(x) = j_L(x) \pm i n_L(x),$$

$j_L$  and  $n_L$  being the spherical Bessel and Neumann functions, respectively.

In the absence of interactions,

$$\frac{1}{r} u_{L'L}^{(+)}(r; p, JST) \rightarrow \delta_{L'L} j_L(pr), \quad (3.13)$$

and the scattering state  $\psi^{(-)}$  reduces to

$$\begin{aligned} \psi_{\mathbf{p}, S M_S T M_T}^{(-)}(\mathbf{r}) &\rightarrow \phi_{\mathbf{p}, S M_S T M_T}(\mathbf{r}) \\ &= \frac{1}{\sqrt{2}} [e^{i\mathbf{p}\cdot\mathbf{r}} - (-)^{S+T} e^{-i\mathbf{p}\cdot\mathbf{r}}] \chi_{M_S}^S \eta_{M_T}^T, \end{aligned} \quad (3.14)$$

that is, an antisymmetric plane-wave state. In the actual calculations which have been carried out, the exact  $\psi^{(-)}$  state in Eq. (3.8) is approximated as<sup>25,26</sup>

$$R_\alpha^{ST}(q, \omega) = \frac{1}{3} \sum_{M_J M_S} \int \frac{d\mathbf{p}}{(2\pi)^3} \frac{1}{2} |A_\alpha^{ST}(\mathbf{q}\mathbf{p}; M_J M_S)|^2 \times \delta(\omega + m_d - (q^2 + m_p^2)^{1/2}), \quad (3.17)$$

with  $A_\alpha^{ST}$  defined as

$$A_\alpha^{ST}(\mathbf{q}\mathbf{p}; M_J M_S) = \langle \mathbf{q}; \mathbf{p}, S M_S T, M_T = 0 | O_\alpha(\mathbf{q}) | d, 1M_J \rangle. \quad (3.18)$$

Here the states  $|d, 1M_J\rangle$  and  $|\mathbf{q}; \mathbf{p}, SM_S TM_T\rangle$  are described by the wave functions (3.5) and (3.6) [with the approximation (3.15)], respectively. In Eq. (3.17),  $m_d$  is the deuteron mass, while the internal energy of the recoiling pair of nucleons is taken to be

$$R_\alpha^{ST}(q, \omega) = \frac{1}{48\pi^2} p m_N \left[ 1 + \frac{\omega + E_d}{2M_N} \right] \sum_{M_J M_S} \int_{-1}^{+1} d(\cos\theta_p) |A_\alpha^{ST}(q, p, \cos\theta_p; M_J M_S)|^2, \quad (3.20)$$

$$p = \frac{1}{2} [(\omega + E_d)(\omega + E_d + 4m_N) - q^2]^{1/2}, \quad (3.21)$$

where  $E_d$  is the deuteron binding energy ( $E_d = -2.225$  MeV) and  $\theta_p$  is the angle between  $\mathbf{q}$  and  $\mathbf{p}$ . By using the partial-wave expansion for  $\psi^{(-)}$ , the standard expressions for  $R_\alpha(q, \omega)$  in terms of charge, electric, and magnetic multipoles are recovered. In the deuteron threshold electrodisintegration at backward angles, the contribution to the cross section from charge scattering is neglected.

For elastic scattering, the relevant amplitudes are given by

$$A_\alpha(\mathbf{q}; M_J' M_J) = \langle \mathbf{q}; d, 1M_J' | O_\alpha(\mathbf{q}) | d, 1M_J \rangle, \quad (3.22)$$

and from these the charge ( $G_0$ ), magnetic ( $G_1$ ), and quadrupole ( $G_2$ ) form factors are easily obtained. For example, we find

$$G_0(q) = \frac{2}{3} \text{Re}[\frac{1}{2} A_L(\mathbf{q}; 00) + A_L(\mathbf{q}; 11)], \quad (3.23)$$

$$G_2(q) = \text{Re}[A_L(\mathbf{q}; 00) - A_L(\mathbf{q}; 11)]/q^2, \quad (3.24)$$

with the normalizations

$$G_0(0) = 1, \quad G_2(0) = \frac{1}{2} Q_d. \quad (3.25)$$

Here  $Q_d$  is the deuteron quadrupole moment.

The initial- and final-state wave functions are written as vectors in the spin-isospin space of the two nucleons for any given spatial configuration  $\mathbf{r}$ . For the given  $\mathbf{r}$  we calculate the state vectors  $O_\alpha(\mathbf{q})|d; 1M_J\rangle$  with the same methods used in the variational Monte Carlo calculations of the charge and magnetic form factors of the three- and four-body nuclei.<sup>13,24</sup> The momentum-dependent terms in  $O_\alpha$ , such as those associated with the convection or spin-orbit current, are calculated numerically. For example,

$$\nabla_\alpha \psi_{d, 1M_J}(\mathbf{r}) = \frac{1}{2\delta_\alpha} [\psi_{d, 1M_J}(\mathbf{r} + \delta_\alpha) - \psi_{d, 1M_J}(\mathbf{r} - \delta_\alpha)], \quad (3.26)$$

where  $\delta_\alpha$  is a small increment in the  $\alpha$  component of  $\mathbf{r}$ . The  $\mathbf{r}$  integration required to calculate the amplitudes is then carried out with conventional numerical techniques. Finally, for the electrodisintegration, the additional  $\theta_p$  integration [Eq. (3.20)] is performed by means of Gaussian quadrature.

The computer program has been tested successfully by comparing the impulse-approximation (IA) results for electrodisintegration into the  $^1S_0$ ,  $^1P_1$ ,  $^3P_0$ , and  $^3S_1$ - $^3D_1$  states with the corresponding ones obtained by using the

$$m_p = 2(p^2 + m_N^2)^{1/2}, \quad (3.19)$$

in order to approximately account for the effects of relativistic kinematics. By integrating out the energy-conserving  $\delta$  function we find

explicit expressions for these contributions in terms of electric and magnetic multipoles as given by Lock and Foldy, Ref. 27. We have also checked that the contributions associated with the generalized pion-exchange and  $\rho$ -meson-exchange currents are correctly calculated for the  $^1S_0$  state, by comparing them with those obtained by Riska, Ref. 17.

#### IV. CROSS SECTION FOR ELECTRODISINTEGRATION AND RADIATIVE CAPTURE

The main component of the cross section for backward electrodisintegration of the deuteron near threshold is the  $M1$  transition between the bound deuteron and the  $^1S_0$  scattering state.<sup>16</sup> At large values of momentum transfer this transition rate is dominated by the exchange-current contribution. The corrections from higher partial waves in the final scattering state are much smaller.<sup>28</sup> Here we take into account all partial waves in the final state, with full account of the strong interaction in the relative  $S$ ,  $P$ , and  $D$  waves, as discussed in the previous section. We have verified to our satisfaction that the numerical importance of the final-state interaction in the higher partial waves is negligible.

In Fig. 3 we compare the calculated cross section for backward electrodisintegration with the empirical values given in Refs. 4 and 29–31. In this figure both the data and the theoretical results have been averaged over the intervals 0–3 and 0–10 MeV of the recoiling  $np$  pair center-of-mass energy for the Saclay ( $q \leq 1$  GeV/c)<sup>29,30</sup> and Stanford Linear Accelerator Center (SLAC) ( $q > 1$  GeV/c)<sup>4</sup> kinematical regions, respectively. In the figure, the results obtained in the impulse approximation and, in addition, with the inclusion of only the “model-independent” exchange-current contributions corresponding to the Argonne  $v_{14}$  potential are shown separately. It is obvious that the “model-dependent” exchange-current contribution represents no more than a minor correction, which improves the calculated results in the region of  $20 \text{ fm}^{-2}$ . The theoretical predictions displayed in Fig. 3 were obtained with the IJL parametrization<sup>8</sup> of the electromagnetic form factors of the nucleon.

Figure 4 is meant to illustrate the sensitivity of the predicted cross section to the electromagnetic form factors of the nucleon: the four curves correspond to the IJL (same as in Fig. 3), Höhler *et al.* (Ref. 9), GK (Ref. 10),

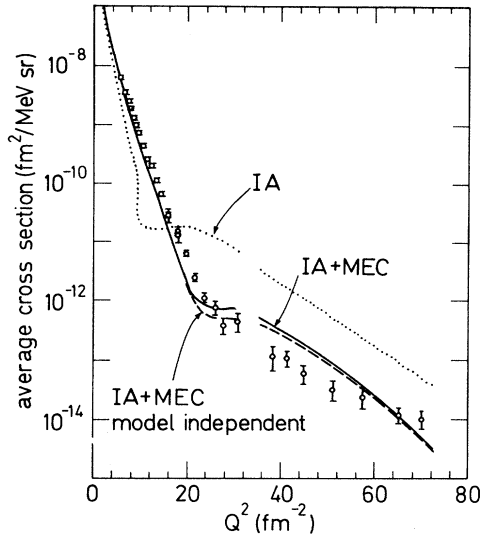


FIG. 3. The cross section for backward electrodisintegration of the deuteron near threshold as obtained with the IJL parametrization<sup>8</sup> of the nucleon electromagnetic form factors. The results calculated in impulse approximation (IA) are displayed along with those obtained with inclusion of the model-independent (IA+MEC model-independent) and both model-independent and model-dependent (IA+MEC) exchange-current contributions. The gap in the figure corresponds to the shift between the Saclay and SLAC center-of-mass energy averages.

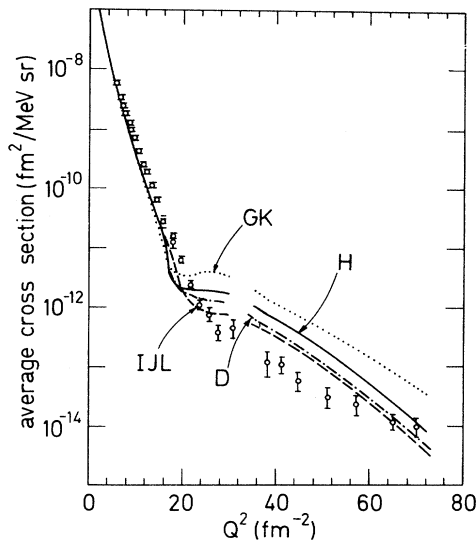


FIG. 4. The cross section for backward electrodisintegration of the deuteron near threshold as obtained with the IJL,<sup>8,9</sup> GK,<sup>10</sup> and D (Ref. 11) parametrizations of the nucleon electromagnetic form factors. All curves include the exchange-current contributions.

and D [with inclusion of the neutron charge form factor (2.2), Ref. 11] parametrizations. It should be noted that the large uncertainty in the behavior of the nucleon electromagnetic form factors (far larger than that in the experimental data) prevents definitive quantitative predictions to be made for  $q > 1$  GeV/c. In this context we emphasize that the isovector Sachs form factor  $G_E^V(q)$  is used in the model-independent isovector exchange-current operator, as required by current conservation and with the further justification that, by using it in place of the Dirac form factor  $F_1^V(q)$ , a transverse relativistic correction from the Pauli term in the amplitude for electroproduction of virtual mesons is automatically included.<sup>12</sup> Indeed, as Fig. 5 shows, much poorer agreement with the data is obtained by using  $F_1^V(q)$  rather than  $G_E^V(q)$ , consistent with what was found in the calculation of the magnetic form factors of the trinucleons, Refs. 7 and 13. It should be mentioned here that previous calculations of the electrodisintegration cross section<sup>3,6</sup> carried out with the Paris potential<sup>2</sup> and essentially the same model for the (dominant) isovector exchange-current operators (that is, constructed to be consistent with the Paris potential) have not come close to the data unless using the  $F_1^V(q)$  parametrization, thus demonstrating that the observable under consideration is directly sensitive to the interaction model through the exchange-current operator. In fact, the isospin-dependent pseudoscalar and vector ("generalized pion and  $\rho$ -meson") components of the Argonne  $v_{14}$  are significantly stronger than those of the Paris potential.<sup>13</sup>

In Fig. 6 we display the contributions to the electrodisintegration cross section from the individual spin-isospin channels of the final scattering state. It is evident that

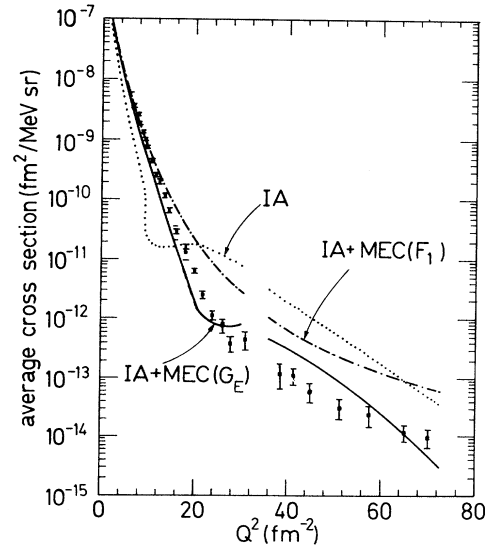


FIG. 5. The cross section for backward electrodisintegration of the deuteron near threshold as obtained by using the IJL (Ref. 8)  $G_E^V(q)$  or  $F_1^V(q)$  nucleon electromagnetic form factors in the isovector model-independent exchange-current operators.

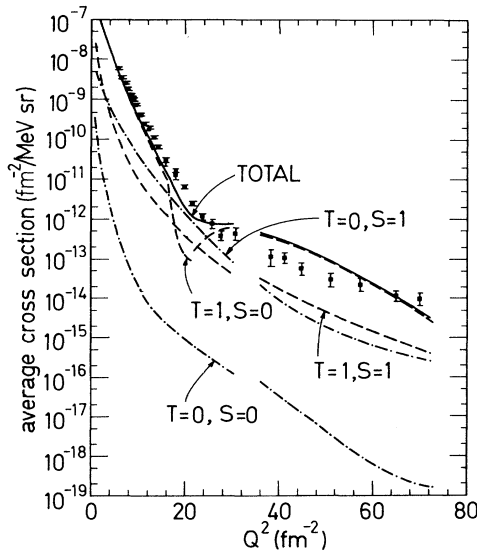


FIG. 6. The contributions to the backward electrodisintegration cross section of the deuteron near threshold from transitions to the different isospin ( $T$ ) and spin ( $S$ ) channels of the final scattering state. The IJL parametrization<sup>8</sup> of the nucleon electromagnetic form factors is used.

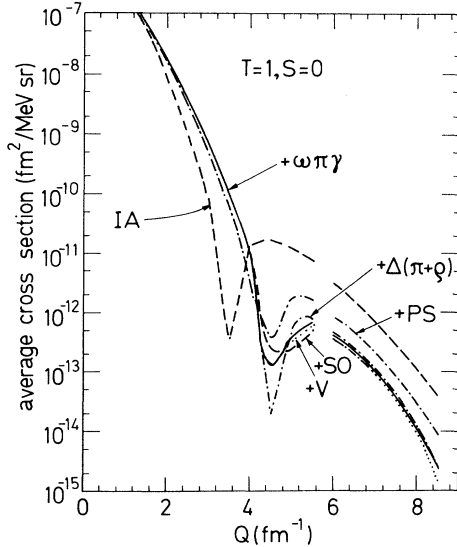


FIG. 7. The individual contributions to the backward electrodisintegration cross section of the deuteron near threshold from transitions to the  $T=1$  and  $S=0$  final states, as obtained with the IJL parametrization<sup>8</sup> of the nucleon electromagnetic form factors. The contributions due to the single-nucleon current (IA), and to the exchange currents associated with the pseudoscalar (PS) and vector (V) parts of the isospin-dependent tensor, and spin-orbit (SO) components of the Argonne  $v_{14}$  interaction, and with the  $\Delta_{33}$  excitation and  $\omega\pi\gamma$  mechanisms are displayed. Note that they are added successively to the IA results in the order stated above.

the  $T=1$  and  $S=0$  channels give the dominant contribution except in the region around  $20 \text{ fm}^{-2}$ , where the destructive interference between the transitions from the  $S$ - and  $D$ -wave components of the deuteron state makes it small. The next most important contributions are those associated with the  $T=0,1$  spin-triplet channels, which substantially increase the cross section in the  $20\text{-fm}^{-2}$  region, bringing it closer to the data. The contribution due to the spin- and isospin-singlet channel is found to be completely negligible.

In Figs. 7–10 we show the contributions to the transition rates in the four separate spin and isospin channels of the final state due to the single-nucleon current (IA), the model-independent exchange currents associated with the pseudoscalar (PS) and vector (V) parts of the isospin-dependent tensor component, and the spin-orbit (SO),  $L^2$  (LL) and quadratic spin-orbit (SO2) components of the Argonne interaction, and finally those due to the model-dependent exchange currents that involve excitation and deexcitation of intermediate virtual  $\Delta_{33}$  resonances through pion and  $\rho$ -meson exchanges [ $\Delta(\pi+\rho)$ ], and the  $\omega\pi\gamma$  ( $\omega\pi\gamma$ ) and  $\rho\pi\gamma$  ( $\rho\pi\gamma$ ) mechanisms (the different corrections are added successively in this order). It should be noted that the PS, V,  $\Delta(\pi+\rho)$ , and  $\omega\pi\gamma$  operators are pure isovector, and therefore their contributions to transitions to the  $T=0$  and  $S=0,1$  channels vanish. Furthermore, the  $\rho\pi\gamma$  current is isoscalar, and its contri-

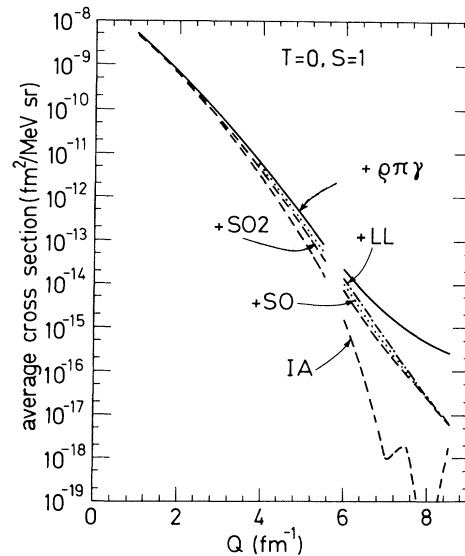


FIG. 8. The individual contributions to the backward electrodisintegration cross section of the deuteron near threshold from transitions to the  $T=0$  and  $S=1$  final state, as obtained with the IJL parametrization<sup>8</sup> of the nucleon electromagnetic form factors. The contributions due to the single-nucleon current (IA), and to the exchange currents associated with the spin-orbit (SO),  $L^2$  (LL), and quadratic spin-orbit (SO2) components of the Argonne  $v_{14}$  interaction, and the  $\rho\pi\gamma$  mechanism are displayed. Note that they are added successively to the IA results in the order stated above.

TABLE I. The  $np \rightarrow d\gamma$  cross section obtained with the single-nucleon current operator (IA), the model-independent exchange currents associated with the pseudoscalar (PS) and vector (V) parts of the isospin-dependent tensor and spin-orbit (SO) components of the Argonne  $v_{14}$  interaction, and with the model-dependent  $\Delta(\pi+\rho)$  and  $\omega\pi\gamma$  mechanisms. The different contributions are added successively in the order stated above.

Current component	Cumulative cross section (mb)
IA	304.1
+PS	322.7
+V	326.1
+SO	326.9
+ $\Delta(\pi+\rho)$	330.1
+ $\omega\pi\gamma$	331.4
Experimental value	$334.2 \pm 0.5$

bution is nonzero only in transitions to the  $T=0$  and  $S=0,1$  channels, while the  $LL$  and  $SO2$  operators are diagonal in the nucleon pair spin states, and therefore their matrix elements between the deuteron ( $S=1$ ) and the

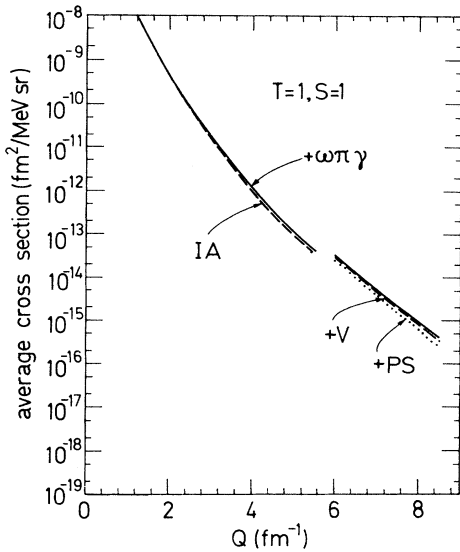


FIG. 9. The individual contributions to the backward electrodisintegration cross section of the deuteron near threshold from transitions to the  $T=1$  and  $S=1$  final states, as obtained with the IJL parametrization<sup>8</sup> of the nucleon electromagnetic form factors. The contributions due to the single-nucleon current (IA), and to the exchange currents associated with the pseudoscalar (PS) and vector (V) parts of the isospin-dependent tensor component of the Argonne  $v_{14}$  interaction, and with the  $\omega\pi\gamma$  mechanism are displayed. Note that they are added successively to the IA results in the order stated above. The  $+\omega\pi\gamma$  curve also includes the very small exchange-current contributions associated with the spin-orbit,  $L^2$ , and quadratic spin-orbit components of the Argonne  $v_{14}$  interaction, and the  $\Delta_{33}$  excitation mechanism.

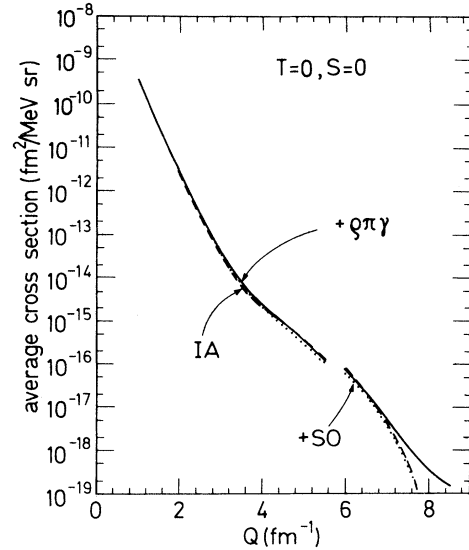


FIG. 10. The individual contributions to the background electrodisintegration cross section of the deuteron near threshold from transitions to the  $T=0$  and  $S=0$  final states, as obtained with the IJL parametrization<sup>8</sup> of the nucleon electromagnetic form factors. The contributions due to the single-nucleon current (IA), and to the exchange currents associated with the spin-orbit (SO) component of the Argonne  $v_{14}$  interaction, and the  $\rho\pi\gamma$  mechanism are displayed. Note that they are added successively to the IA results in the order stated above.

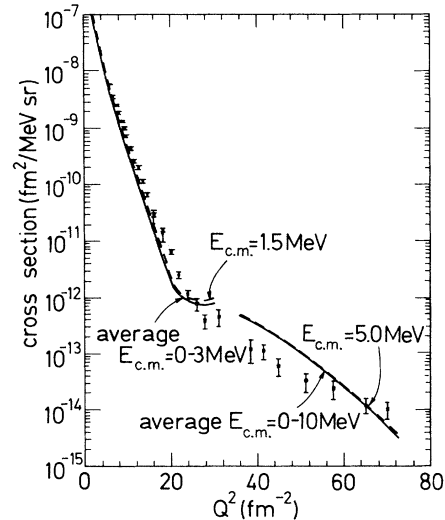


FIG. 11. The threshold electrodisintegration cross sections of the deuteron near threshold calculated at the  $np$  pair center-of-mass energies 1.5 and 5.0 MeV are compared with those obtained by averaging over the center-of-mass energy intervals 0–3 and 0–10 MeV, respectively. The experimental data correspond to the cases of averaging over the intervals 0–3 MeV (low-momentum-transfer region, Refs. 29 and 39) and 0–10 MeV (high-momentum-transfer region, Ref. 4).



$T=0,1$  and  $S=0$  scattering states vanish because of the spin-state orthogonality. Finally, it should be noted that the V contribution also includes a very small correction due to the central isospin-dependent component of the Argonne  $v_{14}$  potential.

For the  $T=1$  and  $S=0,1$  channels, the PS and V operators give the most important and next most important exchange current contributions. The exchange currents due to the momentum dependence of the  $v_{14}$  (SO, LL, and SO2), and the  $\rho\pi\gamma$  mechanism give small corrections to the IA predictions in the  $T=0$  and  $S=0,1$  channels (these corrections, however, become significant at large values of momentum transfer).

Finally, in Fig. 11 we compare the electrodisintegration cross sections calculated at  $E_{c.m.}=1.5$  and 5.0 MeV with those obtained by averaging over the  $E_{c.m.}$  intervals 0–3 and 0–10 MeV, as for the kinematics of the Saclay<sup>29,30</sup> and SLAC (Ref. 4) experiments, respectively. Hence, the effect of the width of the energy interval above threshold of the final state over which the cross-section values are averaged is very small.

The cross section for threshold electrodisintegration is closely related to that for the radiative capture of thermal neutrons on protons (the required matrix elements are connected to each other by time reversal). This radiative capture reaction, which proceeds entirely through the  $^1S_0$  scattering state, in fact provided one of the first convincing cases of a substantial calculable exchange current effect in a photonuclear reaction.<sup>15</sup> In Table I we give the values for the (successive) contributions to this cross section from the different components of the current operator as obtained with the Argonne  $v_{14}$  potential and the present model for the current operator. The impulse-approximation and total cross-section values predicted here are 304.1 and 331.4 mb, respectively. The latter is less than 1% below the empirical value  $334.2 \pm 0.5$  mb,<sup>31</sup> and should thus be viewed as satisfactory. In comparison to the original evaluation of the exchange-current correction in Ref. 15, we find a rather small contribution from the exchange currents that involve excitation of intermediate  $\Delta_{33}$  resonances. This smaller contribution is a consequence of the large cancellation between the pion-exchange-current and  $\rho$ -meson-exchange-current operators that involve the  $\Delta_{33}$  resonance, and the use of the measured transition moment<sup>32</sup> in place of its static quark-model prediction at the  $\gamma N\Delta$  vertex (the former is about 30% smaller than the latter). The satisfactory numerical result for the cross section provides a measure of the quality of the exchange-current operator.

## V. DEUTERON ELECTROMAGNETIC FORM FACTORS

The basic electromagnetic form factors of the deuteron are the charge, quadrupole, and magnetic form factors  $G_C(q)$ ,  $G_Q(q)$ , and  $G_M(q)$ .<sup>21</sup> More closely related to the empirical observables are the  $A(q)$  and  $B(q)$  structure functions which are defined as<sup>33</sup>

$$A(q) = G_C^2(q) + \frac{2}{3}\eta G_M^2(q) + \frac{8}{9}\eta^2 G_Q^2(q), \quad (5.1a)$$

$$B(q) = \frac{4}{3}\eta(\eta+1)G_M^2(q), \quad (5.1b)$$

where  $\eta = q^2/4m_d^2$ . Here  $G_C$ ,  $G_Q$ , and  $G_M$  are normalized as  $G_C(0)=1$ ,  $G_Q(0)=Q_d m_d^2$ , and  $G_M(0)=m_d \mu_d / m_N$ , respectively. The observable that separates the charge and quadrupole form factors is the tensor polarization  $t_{20}(q)$ , defined as<sup>34</sup>

$$t_{20}(q) = -\sqrt{2} \frac{x(x+2)+y/2}{1+2(x^2+y)}, \quad (5.2)$$

where the variables  $x$  and  $y$  are defined as

$$x = \frac{2}{3}\eta \frac{G_Q(q)}{G_C(q)}, \quad (5.3)$$

$$y = \frac{2}{3}\eta \left[ \frac{G_M(q)}{G_C(q)} \right]^2 f(\theta). \quad (5.4)$$

The auxiliary function  $f(\theta)$  is  $\frac{1}{2} + (1+\eta)\tan^2\theta/2$ .

In Fig. 12 we show the predicted charge form factor as a function of momentum transfer. The calculation is based on the Argonne  $v_{14}$  potential and the Höhler *et al.* parametrization<sup>9</sup> for the electromagnetic form factors of the nucleon. The effect of the exchange-charge operators is to bring the zero in the form factor predicted in the impulse approximation towards lower values of momentum transfer. The main exchange correction is that due to the

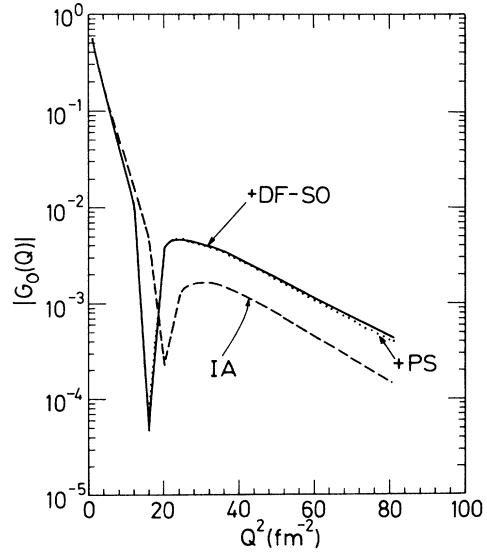


FIG. 12. Individual contributions to the charge form factor of the deuteron as obtained with the Höhler *et al.*<sup>9</sup> parametrization of the nucleon electromagnetic form factors. The contributions due to the single-nucleon (IA) and the PS (“generalized pion”) meson-exchange-charge operators are displayed along with those associated with the Darwin-Foldy and spin-orbit corrections (DF-SO). Note that they are added successively to the IA results in the order stated above. The curve DF-SO also includes the very small contributions due to the V (“generalized  $\rho$ -meson”),  $\omega$ -meson, and  $\rho\pi\gamma$  exchange-charge operators.

pseudoscalar (“generalized pion”) exchange-charge operator. Adding the corrections due to the vector meson-exchange-charge operators and to the Darwin-Foldy and spin-orbit terms in the single-nucleon charge operator amounts to only a very small additional contribution.

In Fig. 13 we show the predicted quadrupole form factor (normalized to  $Q_d/2$ ) as obtained with the Höhler *et al.* parametrization for the electromagnetic form factors of the nucleon. In this case there is a cancellation between the contributions due to the pseudoscalar and vector (“generalized  $\rho$ -meson”) exchange-charge operators. The correction due to the  $\omega$ -meson-exchange-charge operator serves to cancel most of the remainder of the exchange-charge contribution. The Darwin-Foldy and spin-orbit corrections are also small so that, in the case of the quadrupole form factor, the impulse approximation is quite good. (The value for  $Q_d$  obtained with the Argonne  $v_{14}$  interaction is  $Q_d=0.286$  fm<sup>2</sup>; the exchange-charge-operator contributions to this quantity are negligible.)

These results for the charge and quadrupole form factors are qualitatively similar to earlier ones obtained with simple meson-exchange-charge operators and deuteron wave functions that correspond to alternative potential models.<sup>33,35,36</sup> The important role of the exchange-charge operators in bringing the zero in the charge form

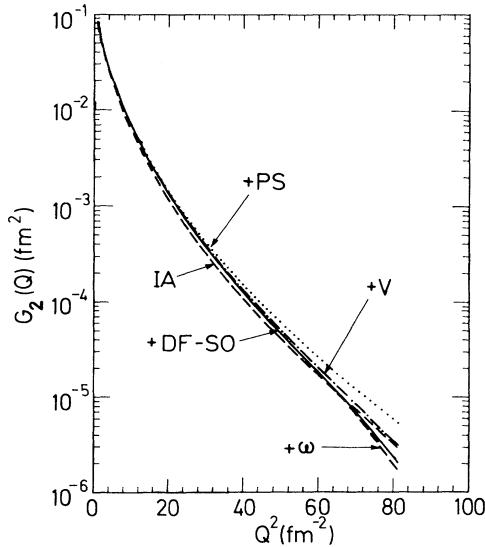


FIG. 13. Individual contributions to the quadrupole form factor of the deuteron as obtained with the Höhler *et al.*<sup>9</sup> parametrization of the nucleon electromagnetic form factors. The contributions due to the single-nucleon (IA), and the PS (“generalized pion”), V (“generalized  $\rho$ -meson”), and  $\omega$ -meson exchange-charge operators are displayed along with those associated with the Darwin-Foldy and spin-orbit corrections (DF-SO). Note that they are added successively to the IA results in the order stated above. The curve DF-SO also includes a very small contribution due to the  $\rho\pi\gamma$  charge operator.

factor towards a lower value of momentum transfer is similar to that in the case of the bound three- and four-nucleon systems, where this effect is required for agreement with the empirical charge form factors.<sup>22–24</sup>

Rather than presenting results for the magnetic form factor  $G_M(q)$ , we shall give predictions for the structure function  $B(q)$ , which is related to  $G_M(q)$  via Eq. (5.1b). In Fig. 14 we show the calculated values for  $B(q)$  as obtained in the impulse approximation and with inclusion of the isoscalar exchange-current contributions of Sec. II (IA+EC). The data points in this and the following figures have been taken from Refs. 37–48. The effect of including the exchange-current contributions improves the fit at low values of momentum transfer, but leads to an overprediction at high momentum transfer, where the impulse-approximation results are too small. Most of this overprediction can be ascribed to the estimate of the very model-dependent  $\rho\pi\gamma$  mechanism, the magnitude of which is far from certain. The results in Fig. 14 were obtained with the Höhler *et al.*<sup>9</sup> parametrization for the electromagnetic form factors of the nucleon. However, the sensitivity to the nucleon form-factor parametrization is not very large, as is evident from Fig. 15 where the results obtained with the IJL (Ref. 8), GK (Ref. 10), and D (Ref. 11) parametrizations are also displayed.

The individual contributions to the structure function  $B(q)$  from the different components of the current operator are shown in Fig. 16. It is evident that the exchange-current operator that is associated with the spin-orbit interaction gives a significant positive contribution to the structure function. This correction here thus has the opposite sign from that obtained in Ref. 49. However, the spin-orbit exchange current used in the present work in

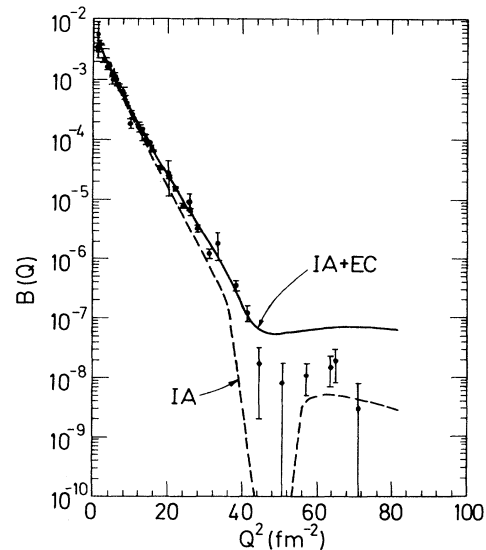


FIG. 14. The deuteron  $B$  structure function in the impulse approximation (IA) and with the inclusion of the exchange-current contributions (IA+EC). The Höhler *et al.*<sup>1</sup> parametrization of the nucleon electromagnetic form factors is used.

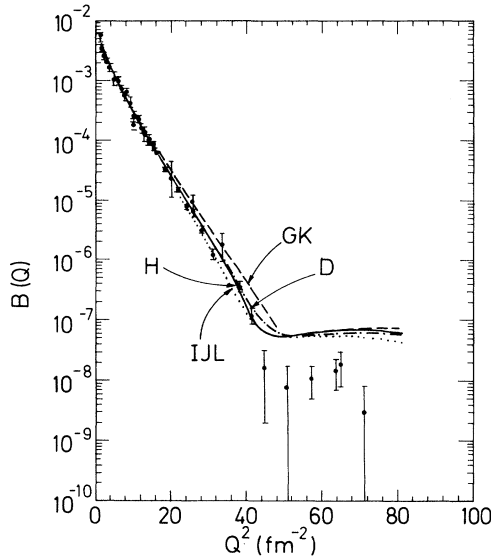


FIG. 15. The deuteron  $B$  structure function as obtained with the IJL, H,<sup>9</sup> GK,<sup>10</sup> and D (Ref. 11) parametrizations of the nucleon electromagnetic form factors. All curves include the exchange-current contributions.

contrast to that employed in Ref. 49 satisfies the continuity equation with the corresponding central and spin-orbit components of the potential, when the single-nucleon charge operator that appears in the continuity

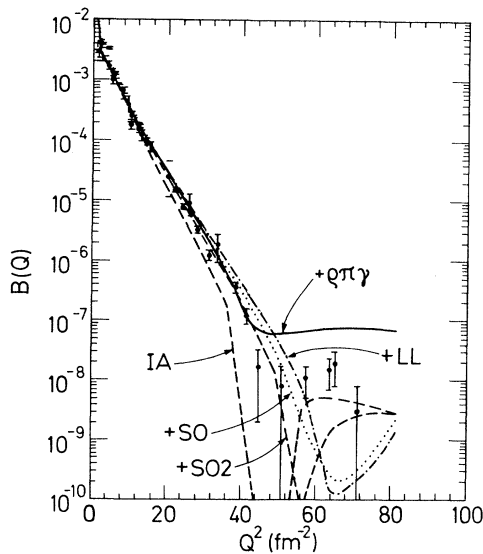


FIG. 16. The individual contributions to the deuteron  $B$  structure function as obtained with the Höhler *et al.*<sup>9</sup> parametrization of the nucleon electromagnetic form factors. The contributions due to the single-nucleon current (IA) and the exchange currents associated with the spin-orbit (SO),  $L^2$  (LL), and quadratic spin-orbit (SO2) components of the Argonne  $v_{14}$  interaction, and the  $\rho\pi\gamma$  mechanism are displayed. Note that they are added successively to the IA results in the order stated above.

equation includes the relativistic corrections proportional to  $m_N^{-2}$ . The importance of taking into account these corrections in the continuity equation has been emphasized by Blunden<sup>18</sup> and Ichii *et al.*<sup>50</sup> The contributions from the exchange-current operators associated with the  $L^2$  and quadratic spin-orbit interactions have opposite signs (the latter is negative in agreement with the result found in Ref. 51). Finally, the effect of the  $\rho\pi\gamma$  exchange current mechanism is large and positive, in agreement with earlier calculations<sup>35,36</sup> [because of the recently raised issue of the sign of this effect,<sup>52</sup> we point out that we use the same (conventional) sign for the  $\rho\pi\gamma$  coupling constant as in Ref. 36].

In the evaluation of the  $\rho\pi\gamma$  exchange-current mechanism, we have taken into account the anomalous tensor coupling between the  $\rho$  meson and the nucleon (the explicit expression in momentum-space of this operator is given in the Appendix). The importance of this term was recently stressed in Ref. 53 in a relativistic boson-exchange-model calculation of the deuteron form factors, based on the Bethe-Salpeter equation. As is evident from Fig. 17, the inclusion of the anomalous tensor coupling term substantially reduces the contribution (in the present framework) of the  $\rho\pi\gamma$  exchange-current mechanism at intermediate values of momentum transfer.

It has to be stressed that the magnitude of the  $\rho\pi\gamma$  exchange-current correction can only be estimated within fairly wide uncertainty limits, because there is little information on how to describe its short-range behavior. In Fig. 18 we show how the predictions for the structure

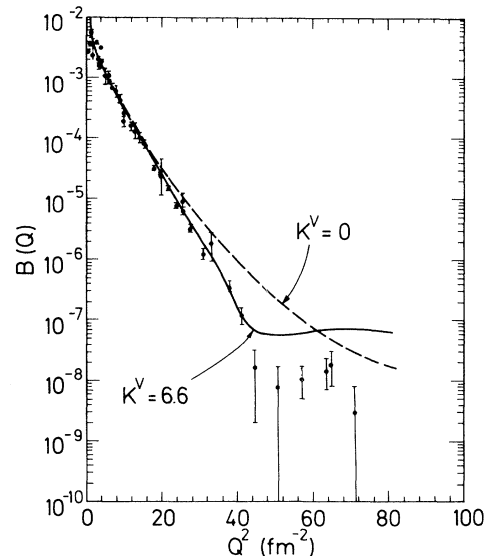


FIG. 17. The  $B$  structure function as obtained with and without taking into account the anomalous  $\rho NN$  tensor coupling constant in the  $\rho\pi\gamma$  exchange current mechanism [Eq. (A2)]. The predicted curves include all other exchange-current contributions. The Höhler *et al.*<sup>9</sup> parametrization of the nucleon electromagnetic form factors is used.

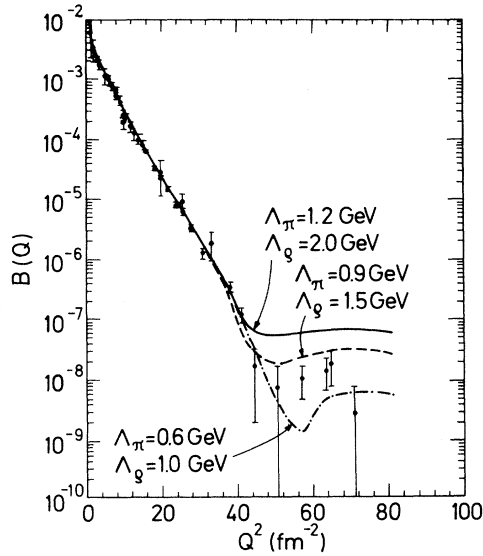


FIG. 18. The effect on the deuteron  $B$  structure function of varying the cutoff mass values in the  $\pi NN$  and  $\rho NN$  vertex form factors of the  $\rho\pi\gamma$  exchange-current operator. The predicted curves include all other exchange-current contributions. The Höhler *et al.*<sup>9</sup> parametrization of the nucleon electromagnetic form factors is used.

function  $B(q)$  change when the cutoff masses at the  $\pi NN$  and  $\rho NN$  vertices in this operator are varied between the two limits  $\Lambda_\pi = 1.2$  GeV/ $c^2$ ,  $\Lambda_\rho = 2.0$  GeV/ $c^2$  and  $\Lambda_\pi = 0.6$  GeV/ $c^2$ ,  $\Lambda_\rho = 1.0$  GeV/ $c^2$ . With the intermediate pair of values  $\Lambda_\pi = 0.9$  GeV/ $c^2$ ,  $\Lambda_\rho = 1.5$  GeV/ $c^2$ , we would obtain an excellent fit to the empirical values over the whole measured range of momentum transfer under the assumption that the form factor has a break in slope but no zero at  $50$  fm $^{-2}$ . An equally good prediction could be obtained by reducing the magnitude of the  $\rho\pi\gamma$  coupling constant from the value  $0.56$  (Ref. 19) to the previously preferred smaller value  $0.4$ .<sup>54</sup>

In Table II we finally give the contributions from the

TABLE II. The deuteron magnetic moment obtained with the single-nucleon current operator (IA), the model-independent exchange currents associated with spin-orbit (SO),  $L^2$  ( $LL$ ), and quadratic spin-orbit (SO2) components of the Argonne  $v_{14}$  interaction, and with the model-dependent  $\rho\pi\gamma$  mechanism. The different contributions are added successively in the order stated above.

Current component	Cumulative magnetic moment ( $\mu_N$ )
IA	0.8453
+SO	0.8636
+LL	0.8682
+SO2	0.8580
+ $\rho\pi\gamma$	0.8638
Experimental value	0.8574

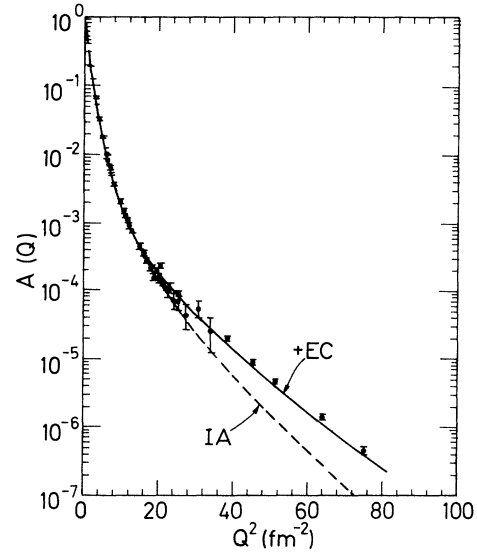


FIG. 19. The deuteron  $A$  structure function in the impulse approximation (IA) and with the inclusion of the exchange-current and -current contributions, as well as the Darwin-Foldy and spin-orbit corrections to the single-nucleon charge operator (+EC). The Höhler *et al.*<sup>9</sup> parametrization of the nucleon electromagnetic form factors is used.

different components of the current operator to the magnetic moment of the deuteron. With the deuteron wave function that corresponds to the Argonne  $v_{14}$  potential model, the impulse-approximation value differs from the

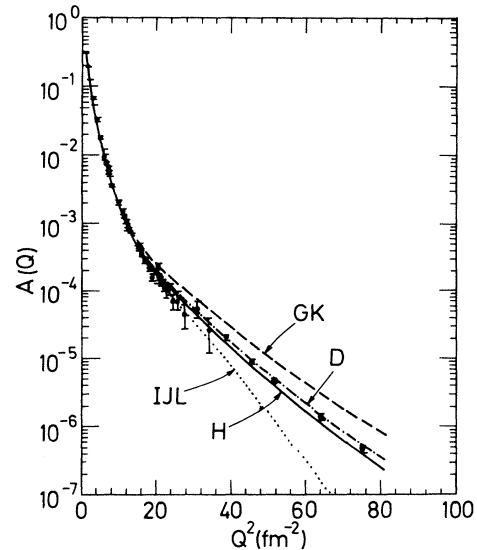


FIG. 20. The deuteron  $A$  structure function as obtained with the IJL,<sup>8</sup> H,<sup>9</sup> GK,<sup>10</sup> and D (Ref. 11) parametrizations of the nucleon electromagnetic form factors. All curves include the meson-exchange contributions and the Darwin-Foldy and spin-orbit corrections to the single-nucleon charge operator.

empirical one by  $0.012\mu_N$ , which amounts to a relative difference of only 1.5%. Adding the exchange-current contributions considered here reduces the magnitude of this difference by half to  $0.0064\mu_N$ . The contribution to the magnetic moment from the  $\rho\pi\gamma$  mechanism is  $0.0058\mu_N$ . Reducing the values of the coupling constant  $g_{\rho\pi\gamma}$  and/or of the cutoff masses in the  $\pi NN$  and  $\rho NN$  vertex form factors would bring the theoretical prediction very close to the empirical value.

In Fig. 19 we show the predictions obtained for the structure function  $A(q)$  [Eq. (5.1a)] using the deuteron wave function that corresponds to the Argonne  $v_{14}$  interaction with and without the exchange-charge and -current contributions. Here the Höhler *et al.*<sup>9</sup> parametrization<sup>9</sup> for the electromagnetic form factors of the nucleon is used and the data points are from Refs. 37, 38, 45, and 55–57. As is illustrated in Fig. 20, the uncertainty in the behavior of the nucleon electromagnetic form factors at large values of momentum transfer produces large differences in the predictions obtained with the IJL, GK, H and D parametrizations. In fact, these differences are larger than those between the IA and IA+MEC results, shown in Fig. 19.

Finally, in Fig. 21 we consider the results for the tensor polarization  $t_{20}(q)$  [Eq. (5.2)], predicted in the impulse approximation and with the inclusion of the contributions from the exchange corrections to the charge and current operators (+EC). The main part of the exchange

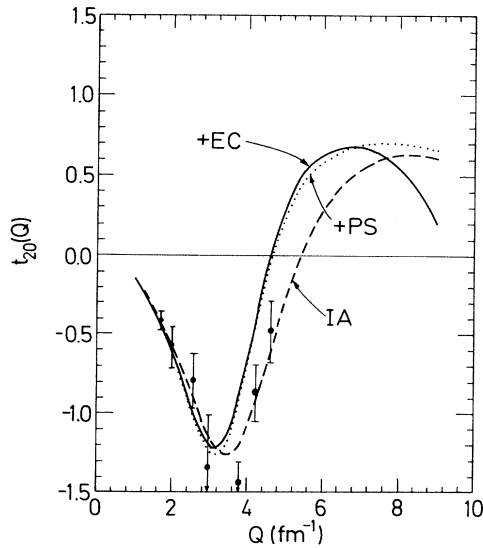


FIG. 21. The deuteron tensor polarization in the impulse approximation (IA) and with the inclusion of the exchange-charge and -current contributions, as well as the Darwin-Foldy and spin-orbit corrections (+EC). The results obtained when the contribution due to the PS (“generalized pion”) exchange-charge operator is added to the impulse approximation are also shown (+PS). The Höhler *et al.*<sup>9</sup> parametrization of the nucleon electromagnetic form factors is used. The data points are from Refs. 34, 58, and 59.

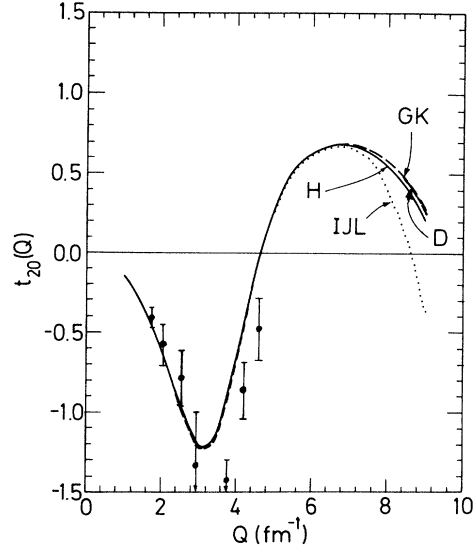


FIG. 22. The deuteron tensor polarization as obtained with the IJL,<sup>8</sup> H,<sup>9</sup> GK,<sup>10</sup> and D (Ref. 11) parametrizations of the nucleon electromagnetic form factors. All curves include the meson-exchange contributions, and the Darwin-Foldy and spin-orbit corrections to the single-nucleon charge operator. The data points are from Refs. 34, 58, and 59.

contributions is that due to the pseudoscalar (“generalized pion”) exchange-charge operator, as shown separately by the curve PS. The curves correspond to setting  $\theta=70^\circ$  in the function  $f(\theta)$  in (5.4). The sensitivity to the electromagnetic form factors of the nucleon is small up to about  $6 \text{ fm}^{-1}$ , as can be seen from Fig. 22. The experimental data in Figs. 21 and 22 have been taken from Refs. 34, 58, and 59. It should be stressed that the last three data points at the highest  $q$  values from Ref. 59 should be considered preliminary.

## VI. DISCUSSION

The two main goals of this work were to test the quality of the Argonne  $v_{14}$  nucleon-nucleon interaction and the accompanying model for the nuclear current operator on the low-energy electromagnetic observables of the two-nucleon system. The importance of this task is obvious as it is a prerequisite for a quantitative theoretical study of the corresponding electromagnetic observables of larger nuclei.

Overall we find that the predicted observables are in fairly good agreement with the empirical values over most of the measured momentum-transfer range. In fact, the predicted static observables, namely, the radiative  $np$  capture cross section and the deuteron magnetic moment, are in excellent agreement with the empirical values. At intermediate values of momentum transfer the present results for the threshold electrodisintegration obtained by using the Argonne  $v_{14}$  potential are, however, not in as good agreement with the empirical values as the very recent results obtained by using an optimal version of the Bonn potential.<sup>5</sup>

The main source of theoretical uncertainty in our results is that associated with the detailed behavior of the electromagnetic form factors of the nucleon. The most common semiempirical parametrizations of these differ widely, especially in the case of the neutron electric form factor. Hence, until this form-factor uncertainty is narrowed, quantitative predictions of electronuclear observables will remain rather tentative. Another source of uncertainty in the present calculations arises from the model-dependent exchange-current mechanisms. The best example of this is the large uncertainty in the predictions for the structure function  $B(q)$  at high values of momentum transfer (Fig. 18), which is due to the unknown short-range behavior of the  $\rho\pi\gamma$  exchange-current mechanism [Fig. 1(c)].

The present investigation of the exchange-current corrections and the quality of the Argonne  $v_{14}$  potential in the two-nucleon electromagnetic observables in a way completes the corresponding studies of the charge and magnetic form factors of the bound three- and four-nucleon systems reported in Refs. 7, 13, and 24. Overall these predictions of the electromagnetic observables of the few-body systems appear to be fairly satisfactory, given the theoretical uncertainty limits mentioned above. Naturally, the nonrelativistic framework used is rather restrictive, and especially at the higher values of momentum transfer explicit relativistic corrections, beyond those considered here, are expected to become appreciable.

#### ACKNOWLEDGMENTS

One of the authors (R.S.) wishes to thank the Nuclear Physics Division of the U.S. Department of Energy under Contract No. W-31-109-ENG-38. The calculations were made possible by grants of time on the Cray supercomputers of the National Energy Research Supercomputer Center of the U.S. Department of Energy.

#### APPENDIX

Here we give the expressions used for the  $\rho\pi\gamma$  exchange-current and -charge operators [Fig. 1(c)]. The  $\rho\pi\gamma$  exchange-current operator contains the term proportional to the  $\rho NN$  tensor coupling constant, which has recently been found to be important.<sup>53</sup>

For the  $\rho\pi\gamma$  exchange-charge operator, we use the usual expression<sup>36</sup>

$$\rho(\mathbf{k}_1, \mathbf{k}_2) = -\frac{f_{\pi NN} g_{\rho\pi\gamma} g_\rho (1+\kappa)}{2m_\pi m_\rho m_N} \tau_1 \cdot \tau_2 \times \left[ \frac{\boldsymbol{\sigma}_1 \cdot \mathbf{k}_1 (\boldsymbol{\sigma}_2 \times \mathbf{k}_2) \cdot (\mathbf{k}_1 \times \mathbf{k}_2)}{(m_\pi^2 + k_1^2)(m_\rho^2 + k_2^2)} - \frac{\boldsymbol{\sigma}_2 \cdot \mathbf{k}_2 (\boldsymbol{\sigma}_1 \times \mathbf{k}_1) \cdot (\mathbf{k}_1 \times \mathbf{k}_2)}{(m_\rho^2 + k_1^2)(m_\pi^2 + k_2^2)} \right]. \quad (\text{A1})$$

Here  $f_{\pi NN}$  is the  $\pi NN$  pseudovector coupling constant,  $g_{\rho\pi\gamma}$  the  $\rho\pi\gamma$  coupling strength, and  $g_\rho$  and  $\kappa$  the  $\rho NN$  vector and tensor couplings. The pion,  $\rho$  meson, and nucleon masses are denoted  $m_\pi$ ,  $m_\rho$ , and  $m_N$ , respectively.

For the  $\rho\pi\gamma$  exchange-current operator we use the expression

$$\mathbf{j} = -i \frac{f_{\pi NN} g_{\rho\pi\gamma} g_\rho}{m_\pi m_\rho} \tau_1 \cdot \tau_2 \frac{\boldsymbol{\sigma}_2 \cdot \mathbf{k}_2 (\mathbf{k}_1 \times \mathbf{k}_2)}{(m_\rho^2 + k_1^2)(m_\pi^2 + k_2^2)} \times \left[ 1 - \frac{k_1^2}{4m_N^2} \left( \frac{1}{2} + \kappa \right) + \frac{i}{8m_N^2} (1 + 2\kappa) \boldsymbol{\sigma}_1 \cdot \mathbf{k}_1 \times (\mathbf{p}_1 + \mathbf{p}'_1) \right] + (1 \leftrightarrow 2). \quad (\text{A2})$$

The terms in this expression proportional to  $m_N^{-2}$  represent relativistic corrections, which would be insignificant if it were not for the large value of the  $\rho NN$  tensor coupling constant  $\kappa$  ( $\kappa = 6.6$ ).

<sup>1</sup>R. B. Wiringa, R. A. Smith, and T. L. Ainsworth, Phys. Rev. C **29**, 1207 (1984).  
<sup>2</sup>M. Lacombe *et al.*, Phys. Rev. C **21**, 861 (1980).  
<sup>3</sup>A. Buchmann, W. Leidemann, and H. Arenhövel, Nucl. Phys. **A443**, 726 (1985).  
<sup>4</sup>R. G. Arnold *et al.*, Phys. Rev. C **42**, 1 (1990).  
<sup>5</sup>W. Leidemann, K.-M. Schmitt, and H. Arenhövel, Phys. Rev. C **42**, 826 (1990).  
<sup>6</sup>S. K. Singh, W. Leidemann, and H. Arenhövel, Z. Phys. A **331**, 509 (1988).  
<sup>7</sup>R. Schiavilla and D. O. Riska, Phys. Lett. B **244**, 373 (1990).  
<sup>8</sup>F. Iachello, A. D. Jackson, and A. Lande, Phys. Lett. **43B**, 191 (1973).  
<sup>9</sup>G. Höhler *et al.*, Nucl. Phys. **B114**, 505 (1976).  
<sup>10</sup>M. Gari and W. Krümpelmann, Phys. Lett. B **173**, 10 (1986).  
<sup>11</sup>C. Ciofi degli Atti, Prog. Part. Nucl. Phys. **3**, 163 (1980).  
<sup>12</sup>D. O. Riska, Phys. Rep. **181**, 207 (1989).  
<sup>13</sup>R. Schiavilla, V. R. Pandharipande, and D. O. Riska, Phys. Rev. C **40**, 2294 (1989).  
<sup>14</sup>J. Carlson, D. O. Riska, R. Schiavilla, and R. B. Wiringa,

Phys. Rev. C **42**, 830 (1990).  
<sup>15</sup>D. O. Riska and G. E. Brown, Phys. Lett. **38B**, 193 (1972).  
<sup>16</sup>J. Hockert, D. O. Riska, M. Gari, and A. Huffman, Nucl. Phys. **A217**, 14 (1973).  
<sup>17</sup>D. O. Riska, Phys. Scr. **31**, 471 (1985).  
<sup>18</sup>P. G. Blunden, Nucl. Phys. **A464**, 525 (1987).  
<sup>19</sup>D. Berg *et al.*, Phys. Rev. Lett. **44**, 706 (1980).  
<sup>20</sup>M. Chemtob and M. Rho, Nucl. Phys. **A163**, 1 (1971).  
<sup>21</sup>T. A. Griffy and L. I. Schiff, in *High Energy Physics*, edited by E. Burhop (Academic, New York, 1967), Vol. 1, p. 341.  
<sup>22</sup>E. Hadjimichael, B. Goulard, and R. Bournais, Phys. Rev. C **27**, 831 (1983).  
<sup>23</sup>W. Strueve, C. Hajduk, P. U. Sauer, and W. Theis, Nucl. Phys. **A465**, 651 (1987).  
<sup>24</sup>R. Schiavilla, V. R. Pandharipande, and D. O. Riska, Phys. Rev. C **41**, 309 (1990).  
<sup>25</sup>R. M. Renard, J. Tran Thanh Van, and M. Le Bellac, Nuovo Cimento **38**, 565 (1965).  
<sup>26</sup>W. Fabian and H. Arenhövel, Nucl. Phys. **A314**, 253 (1979).  
<sup>27</sup>J. A. Lock and L. L. Foldy, Ann. Phys. **93**, 276 (1975).

- <sup>28</sup>W. Leidemann and H. Arenhövel, Nucl. Phys. **A393**, 385 (1983).
- <sup>29</sup>M. Bernheim *et al.*, Phys. Rev. Lett. **46**, 402 (1981).
- <sup>30</sup>S. Auffret *et al.*, Phys. Rev. Lett. **55**, 1362 (1985).
- <sup>31</sup>A. E. Cox, S. A. R. Wynchank, and C. H. Collie, Nucl. Phys. **74**, 497 (1965).
- <sup>32</sup>C. E. Carlson, Phys. Rev. D **34**, 2704 (1986).
- <sup>33</sup>E. L. Lomon, Ann. Phys. **125**, 309 (1980).
- <sup>34</sup>M. E. Schulze *et al.*, Phys. Rev. Lett. **52**, 597 (1984).
- <sup>35</sup>A. D. Jackson, A. Lande, and D. O. Riska, Phys. Lett. **55B**, 23 (1975).
- <sup>36</sup>M. Gari and H. Hyuga, Nucl. Phys. **A264**, 409 (1976).
- <sup>37</sup>D. Benaksas *et al.*, Phys. Rev. **148**, 1327 (1966).
- <sup>38</sup>C. B. Buchanan and M. R. Yearian, Phys. Rev. Lett. **15**, 303 (1965).
- <sup>39</sup>B. Grossetête *et al.*, Phys. Rev. **141**, 1425 (1966).
- <sup>40</sup>R. E. Rand *et al.*, Phys. Rev. Lett. **18**, 469 (1967).
- <sup>41</sup>B. Ganichot *et al.*, Nucl. Phys. **A178**, 545 (1972).
- <sup>42</sup>F. Martin *et al.*, Phys. Rev. Lett. **38**, 1320 (1977).
- <sup>43</sup>E. C. Jones *et al.*, Phys. Rev. C **21**, 1162 (1980).
- <sup>44</sup>G. G. Simon *et al.*, Nucl. Phys. **A364**, 285 (1981).
- <sup>45</sup>R. Cramer *et al.*, Z. Phys. C **29**, 513 (1985).
- <sup>46</sup>S. Auffret *et al.*, Phys. Rev. Lett. **54**, 649 (1985).
- <sup>47</sup>R. G. Arnold *et al.*, Phys. Rev. Lett. **58**, 1723 (1987).
- <sup>48</sup>P. E. Bosted *et al.*, Phys. Rev. C **42**, 38 (1990).
- <sup>49</sup>D. O. Riska, Phys. Scr. **31**, 107 (1985).
- <sup>50</sup>S. Ichii, W. Bentz, and A. Arima, Nucl. Phys. **A464**, 575 (1987).
- <sup>51</sup>D. O. Riska and M. Poppius, Phys. Scr. **32**, 581 (1985).
- <sup>52</sup>P. Sarriguren, J. Martorell, and D. W. L. Sprung, Phys. Lett. **B 228**, 285 (1989).
- <sup>53</sup>E. Hummel and J. A. Tjon, Phys. Rev. Lett. **63**, 1788 (1989).
- <sup>54</sup>M. M. Nagels *et al.*, Nucl. Phys. **B147**, 189 (1979).
- <sup>55</sup>J. E. Elias *et al.*, Phys. Rev. **177**, 2075 (1969).
- <sup>56</sup>S. Galster *et al.*, Nucl. Phys. **B32**, 221 (1971).
- <sup>57</sup>R. Arnold *et al.*, Phys. Rev. Lett. **35**, 776 (1975).
- <sup>58</sup>R. Gilman *et al.*, Phys. Rev. Lett. **65**, 1733 (1990).
- <sup>59</sup>I. The *et al.*, *Proceedings of the PANIC XII International Conference on Particles and Nuclei*, Massachusetts, 1990 (Massachusetts Institute of Technology, Cambridge, Massachusetts, 1990).